Carrier-Mediated Antiferromagnetic Interlayer Exchange Coupling in Diluted Magnetic Semiconductor Multilayers Ga$_{1-x}$Mn$_x$As/GaAs:Be

J.-H. Chung,[1] S. J. Chung,[1] Sanghoon Lee,[1,*] B. J. Kirby,[2] J. A. Borchers,[2] Y. J. Cho,[3] X. Liu,[3] and J. K. Furdyna[3]

[1]*Department of Physics, Korea University, Seoul 136-713, Korea*
[2]*National Institute of Standards and Technology, Gaithersburg, Maryland 20899, USA*
[3]*Department of Physics, University of Notre Dame, Notre Dame, Indiana 46556, USA*

We report the antiferromagnetic (AFM) interlayer exchange coupling between Ga$_{0.97}$Mn$_{0.03}$As ferromagnetic semiconductor layers separated by Be-doped GaAs spacers. Polarized neutron reflectivity reveals a characteristic splitting at the wave vector corresponding to twice the multilayer period, indicating that the coupling between the ferromagnetic layers is AFM. When the applied field is increased to above the saturation field, this AFM coupling is suppressed. This behavior is not observed when the spacers are undoped, suggesting that the observed AFM coupling is mediated by doped charge carriers.

PACS numbers: 75.50.Pp, 61.05.fj, 61.72.uj, 75.25.+z

The exploration of systems that combine electronic and spin degrees of freedom is the subject of major interest in recent semiconductor electronics research. Spin-dependent transport has already demonstrated its technological impact in the form of metallic ferromagnetic multilayers, where giant resistance changes are observed under an external magnetic field [1,2]. A prerequisite for such a large magnetoresistance is the presence of stable antiferromagnetic (AFM) coupling between ferromagnetic (FM) layers, which can be overcome by the application of an applied field [3]. Spin-dependent scattering of charge carriers that changes greatly depending on interlayer exchange coupling (IEC) is the origin of the observed magnetoresistance. Such AFM IEC has been observed in various metallic [4–7] and semiconductor [8–11] multilayers.

Diluted magnetic semiconductors (DMS) in which ferromagnetism is induced via spin-charge doping into III–V semiconductors have been widely studied with an eye on combining spintronics with well-established semiconductor technology. One of the most intensively studied DMS systems is Ga$_{1-x}$Mn$_x$As [12], where the substitutional doping by Mn$'_{Ga}$ results in ferromagnetism mediated by holes [13,14]. Realization of reversible switching between AFM and FM spin states in DMS multilayers may greatly enhance the magnetoresistance in these systems. So far, however, AFM IEC in GaMnAs-based multilayers has never been reported, and only the FM IEC is explicitly observed [15–20]. In principle, AFM IEC is expected to emerge when carrier density is enhanced in the nonmagnetic spacers [21–23]. Several recent experimental studies indeed suggested possible signatures of weak or partial AFM IEC via indirect modulation doping [24,25]. Therefore, it is suspected that carrier doping directly into the spacers has high promise for achieving robust AFM IEC.

In this work, we have used polarized neutron reflectometry to obtain definitive evidence of AFM IEC in a DMS-based multilayer structure Ga$_{0.97}$Mn$_{0.03}$As/GaAs:Be in which the nonmagnetic spacers are doped by Be. Importantly, FM alignment was only observed in the case of a sample with undoped spacers, indicating that the AFM IEC was mediated by charge carriers in the nonmagnetic spacers introduced via Be doping. We show additionally that dc magnetization measurements are also consistent with the IEC described above.

The DMS multilayers used in this study consist of 10 Ga$_{0.97}$Mn$_{0.03}$As layers separated by GaAs spacers, deposited on GaAs (001) substrates by molecular beam epitaxy. Two nearly identical samples were fabricated, one with Be-doped GaAs spacers, the other with undoped spacers. The Be concentration in the spacers is estimated as 1.2×10^{20} cm^{-3} from Hall measurements carried out on a reference sample. A capping layer of undoped GaAs was deposited on top of both multilayers. From neutron reflectivity data (discussed later), the thicknesses of DMS, spacer, and capping layers are determined to be 6.95, 3.47, and 3.47 nm (2.90 nm), respectively, for the Be-doped (undoped) sample.

We begin by presenting the temperature dependences of the magnetization of the multilayers measured using a SQUID vibrating sample magnetometer while cooling. Figure 1 shows the magnetization curves in a series of dc fields applied along the [100] direction, which is approximately parallel to the magnetic easy axis at the lowest temperature. In the sample with undoped spacers, the magnetization increases below $T \approx 60$ K following the typical behavior of ferromagnetic Ga$_{1-x}$Mn$_x$As. A small kink is observed at $T \approx 28$ K, suggesting the development of a biaxial cubic anisotropy [26]. In sharp contrast, in the sample with Be-doped spacers the temperature behavior of magnetization measured in low fields is very different. For instance, the magnetization measured at 4 mT rises around 50 K, then drops as the temperature is lowered to below 40 K, followed by another upturn. At zero field, the net magnetization is almost completely suppressed, showing
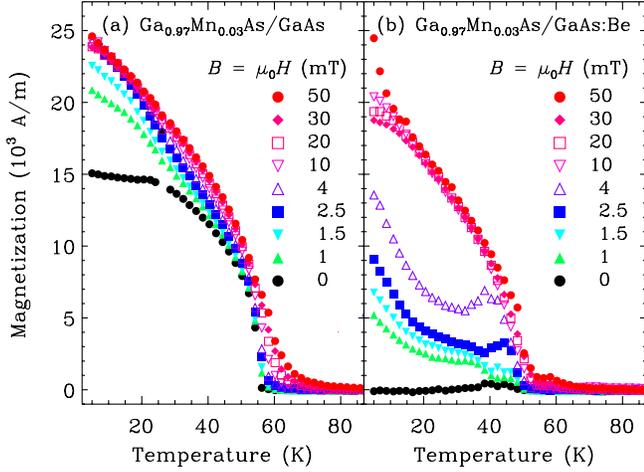
FIG. 1 (color online). Temperature dependence of magnetization of $Ga_{0.97}Mn_{0.03}As/GaAs$ (a) and $Ga_{0.97}Mn_{0.03}As/GaAs{:}Be$ (b) multilayers. The data were collected while cooling, with the magnetic field applied along the [100] direction.

sities for the DMS layers are much weaker (by several orders of magnitude).

The unpolarized neutron reflectivity measured on the Be-doped sample at 100 K (i.e., when the GaMnAs layers are in the paramagnetic phase), plotted in the uppermost part of Fig. 2(a), shows a structural Bragg peak located at ≈ 0.062 Å^{-1}, which corresponds to the multilayer periodicity of ≈ 100 Å. The S-shaped profile of the Bragg peak (instead of a simple peak) is attributed to the presence of a capping layer, a feature that is reproduced by model fitting [28]. The sample was then cooled to 7 K in a field below 0.1 mT, and after cooling down the desired field was applied for measurement. In Fig. 2(a) we show the two NSF reflectivity curves together for each field. The polarized reflectivity data measured at 1.5 mT show that, while the structural Bragg peak was nearly unchanged, a splitting appeared between the two NSF curves at ≈ 0.031 Å^{-1}. This provides a signature that there is an additional periodicity with twice the length of the multilayer period, and

only a very weak signal below T_C. Such a large decrease in net magnetization indicates significant changes in exchange coupling due to Be doping, strongly suggesting that IEC between ferromagnetic layers is antiferromagnetic. In comparison, the magnetization of the multilayers measured at fields higher than 10 mT shows normal FM behavior, suggesting that in these fields IEC is ferromagnetic.

To confirm the presence of the suspected AFM IEC, we performed unpolarized and polarized neutron reflectivity measurements. The experiments were done using the NG-1 polarized beam reflectometer at the NIST Center for Neutron Research. We note that during the polarized reflectivity measurements it was necessary to apply a magnetic field higher than 1 mT in order to maintain high neutron spin polarization ($>$93%). The samples were oriented with the [110] axis parallel to the polarization of a monochromatic neutron beam ($\lambda = 4.75$ Å). Four polarized magnetic scattering intensities were separately measured, from which fully reduced reflectivity curves were obtained [27]. Two non-spin-flip (NSF) structure factors, $(++)$ and $(--)$, are written in the Born approximation as $F^{(\pm\pm)}(Q) = \sum_{j=1}^{N}(b_j \mp p_j\cos\phi_j)e^{iQu_j}$, where b_j and p_j are the nuclear and the magnetic scattering lengths, respectively, ϕ_j is the angle between magnetization vector and applied field, and u_j is the position of the jth atomic plane. The magnetization components parallel to the applied field can then be obtained from the splittings between the two NSF intensities. The spin flip (SF) structure factors, $(+-)$ and $(-+)$, on the other hand, are given by $F^{(\pm\mp)}(Q) = \pm\sum_{j=1}^{N}p_j\sin\phi_j e^{iQu_j}$, and involve magnetization components perpendicular to the applied field. Below we show only the NSF reflection intensities, because the SF inten-
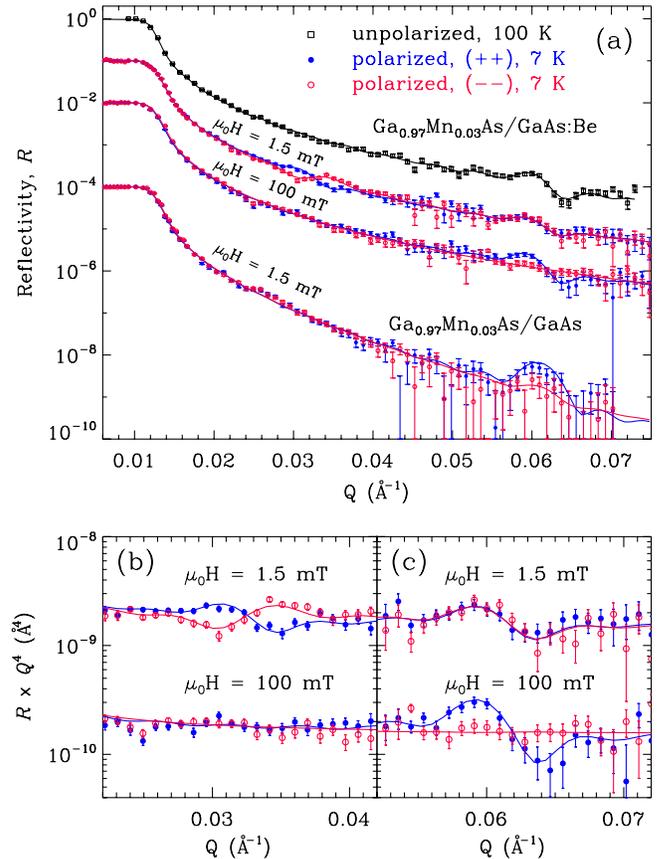

FIG. 2 (color online). (a) Unpolarized and polarized neutron reflectivities of the Be-doped and the undoped multilayers with the field applied along the [110] direction. The curves are shifted vertically for clarity. The solid lines are fits to the data using the models described in the text. The AFM and the FM splittings of the Be-doped sample are emphasized by $R \times Q^4$ curves in (b) and (c), respectively.

it is caused by the spin components parallel or antiparallel to the neutron polarization. It is evident that such magnetic periodicity is consistent with AFM IEC between the DMS layers. Note, however, that this splitting is fully suppressed when the applied field is increased to 100 mT. Instead, a new splitting is observed at the structural Bragg peak, indicating FM saturation. In contrast, the undoped sample shows a splitting of only its structural Bragg peak, even at lowest fields. It indicates that the DMS layers in the undoped sample are aligned ferromagnetically along the applied field. We therefore conclude that IEC in the undoped sample is very different from that in the Be-doped, and is either FM or nearly uncoupled.

Using the REFLPAK program [28], we performed quantitative fitting of the reflectivity curves. The magnetization in the DMS layers was assumed to be uniform. The fitting results, plotted as solid curves in Fig. 2(a), show that the reflectivity measured at the two fields is indeed due to AFM and FM IEC between the ferromagnetic DMS layers, respectively. The splittings in the $R \times Q^4$ curves are amplified in Figs. 2(b) and 2(c). At 100 mT, which is above the saturation field, we obtain the magnetic moment per Mn ion projected along the [110] direction to be $m_{\mathrm{Mn}}^{[110]} = 2.8 \pm 0.3 \mu_B$. The difference with respect to the value $3.2 \mu_B$ previously reported [29] can most probably be ascribed to the presence of interstitial Mn ions, since our samples were not annealed to reduce their concentration [14]. In comparison, we obtain $m_{\mathrm{Mn}}^{[110]} = 2.1 \pm 0.2 \mu_B$ for the AFM-coupled phase at 1.5 mT. The ratio between the observed moments is consistent with the rotation of the easy axis away from the [110] direction by $\eta = 40° \approx \cos^{-1}(2.1/2.8)$ at 7 K [26,30]. However, this rotation does not result in AFM components oriented along the [1$\bar{1}$0] direction, which would have been the case if we were dealing with the rotation of a single AFM domain. We found no observable splittings when the sample was oriented with the [1$\bar{1}$0] direction parallel to the neutron polarization and the same measurement was repeated. We therefore suspect that each DMS layer consists of a distribution of two types of domains whose easy axes are tilted away from [110] by $\pm \eta$, respectively, thus canceling the spin components along [1$\bar{1}$0]. Such behavior also suggests that the sample is likely to form a virtually single domain near T_C, where uniaxial anisotropy is dominant.

We examined the field dependent behavior of the IEC in more detail by measuring the NSF reflection intensities. The plots in Fig. 3 show that, as the applied field is increased at 7 K, the FM splitting is enhanced at the expense of the AFM splitting. The AFM splitting is almost completely suppressed around 10 mT consistent with the magnetization data, but full development of the FM splitting required higher fields. When the field is lowered down to 1 mT directly from full saturation at 100 mT, the AFM splitting does not recover, and only the FM splitting remains. This is ascribed to a lock-in caused by the strong
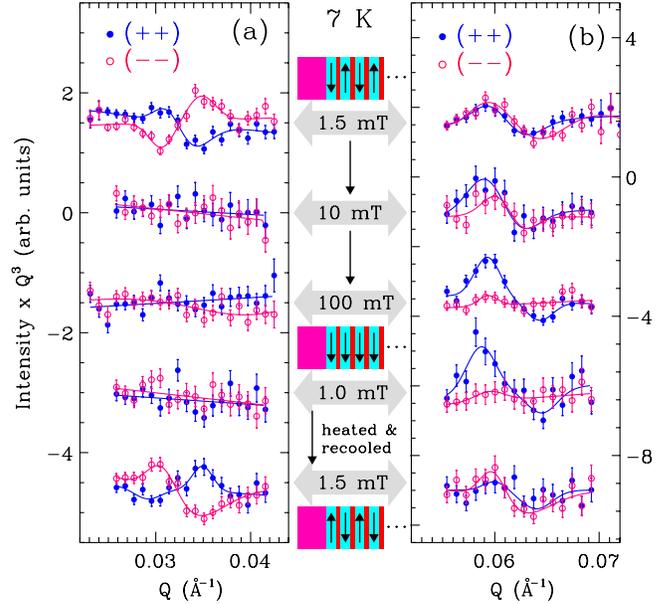

FIG. 3 (color online).   The AFM (a) and the FM (b) splittings in the NSF reflection intensities of the Be-doped sample measured at 7 K. The data were collected sequentially in the order from top to bottom, and corresponding applied fields are shown in the middle. The lines through the data are guides for the eye. The illustrations in the middle column schematically show the spin orientations in the multilayer at corresponding fields.

cubic biaxial anisotropy field at low temperatures [26]. The AFM IEC can be recovered by raising the temperature above T_C and then recooling down to 7 K. We observed that in this process the direction of the splitting can be reversed, i.e., that the interlayer spin correlations can change from ↑↓↑↓ … to ↓↑↓↑ …. This result indicates that the observed AFM IEC is not initiated by some weak remanent field during the cooling, but is truly intrinsic to the sample.

In contrast, when the sample is cooled only to 30 K, the AFM IEC is recovered without a lock-in after field cycling. Figure 4 shows that a nearly identical AFM splitting is observed when the field is raised to 30 mT and lowered back to 1.5 mT. It is because the cubic anisotropy field decreases in strength at higher temperatures, and is not strong enough at 30 K to cause a lock-in of the FM alignment. All these results show that the AFM IEC observed in our sample is stable over the temperature range observed.

In the case of metal-based multilayers, the IEC between the magnetic layers is known to oscillate between AFM and FM as a function of the nonmagnetic spacer thickness [4,5], being induced by RKKY-type interaction through conduction electrons [31]. Since the GaAs is insulating, carrier injection into the spacers is required to expect similar effects. The Be doping in the spacers is known to increase the hole concentrations directly in the GaAs layers [32], as well as in nearby DMS layers [33]. The hole concentration in the GaAs:Be layers in our sample is
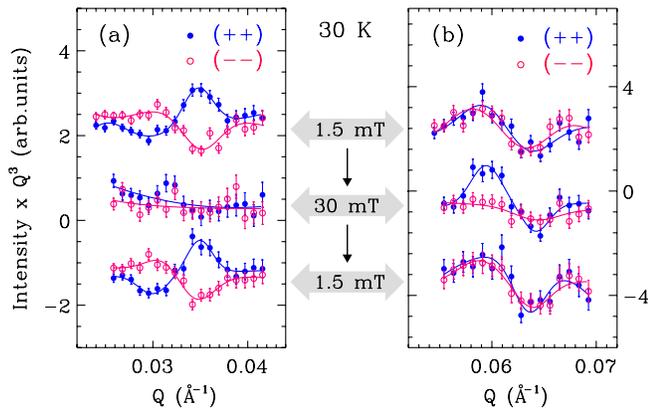
FIG. 4 (color online).   The AFM (a) and the FM (b) splittings in the NSF reflection intensities of the Be-doped sample measured at 30 K.

estimated to be 1.0×10^{20} cm^{-3} at 7 K. Recent theoretical studies predict that IEC in GaMnAs-based multilayers can also be changed from FM to AFM via carrier doping and spacer thickness control [22,23]. In light of these works, however, the discovery of stable AFM IEC in our sample is quite intriguing. The spacers in our sample are as thick as ≈12 monolayers, a thickness for which according to calculations the exchange strength should be very weak. We suspect that in our case the stability of the observed AFM IEC may have been enhanced by the thickness of the DMS layers, which is ≈25 monolayers. Interestingly, a mean field calculation shows that, as the thickness of the DMS layer is increased, the oscillatory behavior of the IEC is changed and becomes less dependent on the spacer thickness [23]. Our result therefore may be indicating that reliable magnetoresistance devices based on DMS multilayers require thicknesses (both for the DMS layers and the spacers) much greater than those typically used for metal-based devices.

In summary, using dc magnetization and polarized neutron reflectometry measurements, we have observed AFM IEC in $Ga_{0.97}Mn_{0.03}As/GaAs$:Be multilayers in which the nonmagnetic GaAs spacers are doped with Be. In sharp contrast, $Ga_{0.97}Mn_{0.03}As/GaAs$ multilayers with no Be doping showed only FM alignment. Our experimental finding is thus an important step toward theoretical and quantitative understanding of IEC between DMS layers separated by nonmagnetic spacers.

*slee3@korea.ac.kr
[1] M. N. Baibich *et al.*, Phys. Rev. Lett. **61**, 2472 (1988).
[2] G. Binasch *et al.*, Phys. Rev. B **39**, 4828 (1989).
[3] P. Grünberg *et al.*, Phys. Rev. Lett. **57**, 2442 (1986).
[4] S. S. Parkin *et al.*, Phys. Rev. Lett. **64**, 2304 (1990).
[5] S. S. Parkin *et al.*, Phys. Rev. Lett. **67**, 3598 (1991).
[6] P. J. Bloemen *et al.*, Phys. Rev. B **50**, 13 505 (1994).
[7] J. A. Borchers *et al.*, Phys. Rev. Lett. **82**, 2796 (1999).
[8] J. J. Rhyne *et al.*, J. Magn. Magn. Mater. **177–181**, 1195 (1998).
[9] H. Kępa *et al.*, Europhys. Lett. **56**, 54 (2001).
[10] H. Kępa *et al.*, Phys. Rev. B **68**, 024419 (2003).
[11] H. Kępa *et al.*, Physica (Amsterdam) **335B**, 44 (2003).
[12] T. Jungwirth *et al.*, Rev. Mod. Phys. **78**, 809 (2006).
[13] B. Beschoten *et al.*, Phys. Rev. Lett. **83**, 3073 (1999).
[14] J. Blinowski and P. Kacman, Phys. Rev. B **67**, 121204(R) (2003).
[15] H. Munekata *et al.*, Phys. Rev. Lett. **63**, 1849 (1989).
[16] H. Ohno *et al.*, Phys. Rev. Lett. **68**, 2664 (1992).
[17] H. Ohno *et al.*, Appl. Phys. Lett. **69**, 363 (1996).
[18] T. Hayashi *et al.*, J. Cryst. Growth **175–176**, 1063 (1997).
[19] H. Kępa *et al.*, Phys. Rev. B **64**, 121302 (2001).
[20] B. J. Kirby *et al.*, Phys. Rev. B **76**, 205316 (2007).
[21] T. Jungwirth *et al.*, Phys. Rev. B **59**, 9818 (1999).
[22] P. Sankowski and P. Kacman, Phys. Rev. B **71**, 201303(R) (2005).
[23] A. D. Giddings *et al.*, Phys. Status Solidi C **3**, 4070 (2006).
[24] Z. Ge *et al.*, Appl. Phys. Lett. **91**, 152109 (2007).
[25] B. J. Kirby *et al.*, J. Appl. Phys. **103**, 07D116 (2008).
[26] D. Y. Shin *et al.*, Phys. Rev. B **76**, 035327 (2007).
[27] C. F. Majkrzak, Physica (Amsterdam) **173B**, 75 (1991).
[28] P. A. Kienzle *et al.*, REFLPAK, http://www.ncnr.nist.gov/reflpak, 2000–2006.
[29] S. J. Potashnik *et al.*, Phys. Rev. B **66**, 012408 (2002).
[30] U. Welp *et al.*, Phys. Rev. Lett. **90**, 167206 (2003).
[31] P. Bruno and C. Chappert, Phys. Rev. Lett. **67**, 1602 (1991).
[32] S. Lee *et al.*, J. Appl. Phys. **93**, 8307 (2003).
[33] T. Wojtowicz *et al.*, Appl. Phys. Lett. **83**, 4220 (2003).